

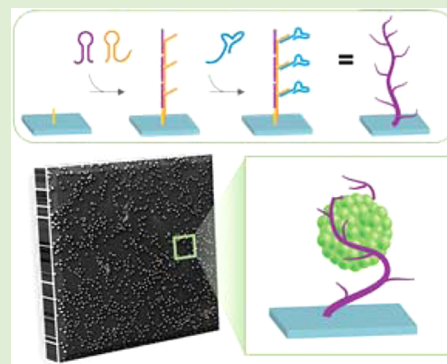
Polymerization of Affinity Ligands on a Surface for Enhanced Ligand Display and Cell Binding

Erin Richards, Shihui Li, Niancao Chen, Mark R. Battig, and Yong Wang*

Department of Biomedical Engineering, The Pennsylvania State University, University Park, Pennsylvania 16802-6804, United States

 Supporting Information

ABSTRACT: Surfaces functionalized with affinity ligands have been widely studied for applications such as biological separations and cell regulation. While individual ligands can be directly conjugated onto a surface, it is often important to conjugate polyvalent ligands onto the surface to enhance ligand display. This study was aimed at exploring a method for surface functionalization via polymerization of affinity ligands, which was achieved through ligand hybridization with DNA polymers protruding from the surface. The surface with polyvalent ligands was evaluated via aptamer-mediated cell binding. The results show that this surface bound target cells more effectively than a surface directly functionalized with individual ligands in situations with either equal amounts of ligand display or equal amounts of surface reaction sites. Therefore, this study has demonstrated a new strategy for surface functionalization to enhance ligand display and cell binding. This strategy may find broad applications in settings where surface area is limited or the surface of a material does not possess sufficient reaction sites.



1. INTRODUCTION

Ligand display on a surface is important for various applications such as separations, biosensing, biomolecular patterning, cell immobilization, and basic life science studies.^{1–5} It is usually achieved via two main strategies: direct conjugation of individual ligands onto an activated surface or conjugation of polyvalent ligands onto the surface. While the former method is straightforward, the latter is often needed in situations where materials are inert (i.e., lack of sufficient reaction sites) or a higher degree of valence is needed. The conjugation of polyvalent ligands on surfaces has been demonstrated by surface functionalization with polymers (e.g., dextran and dendrimers)^{6–8} or nanomaterials (e.g., gold nanoparticles or nanopillars),^{9–11} each of which bears multiple peptides or antibodies. The purpose of this study was to develop and apply a new ligand display method for surface functionalization with nucleic acid-based polyvalent aptamers.

Nucleic acid aptamers are short single-stranded oligonucleotides capable of binding to their targets with high affinities and specificities.^{12,13} They are selected from DNA/RNA libraries^{14,15} in vitro and can be synthesized using chemical methods. Since they consist of nucleotides, they are tolerant of many harsh chemical and physical environments without losing their binding functionalities. Thus, aptamers have been widely studied for nanoparticle delivery, molecular sensing, and controlled growth factor release.^{16–19} Recently, we and several other groups have applied aptamers to functionalize surfaces for cell catch^{20–23} since the ability to catch target cells on a surface is important for clinical diagnoses and regenerative medicine applications.²⁴ While previous results have shown that aptamer-

functionalized surfaces can catch target cells, no effort has been made to examine the difference between individual and polyvalent aptamer-functionalized surfaces in cell catch, which was the focus of this study.

The method for synthesizing polyvalent aptamers on the surface is depicted in Figure 1. The process involves two main

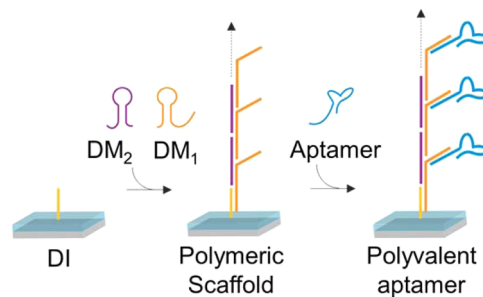


Figure 1. Schematic illustration of DNA polymerization for enhanced display of aptamers.

steps and four different single-stranded oligonucleotides: an initiator (DNA initiator, DI), two monomers [DNA monomer 1 (DM₁) and DNA monomer 2 (DM₂)] and an aptamer (Table 1). The first step is the synthesis of a polymeric DNA scaffold via hybridization chain reaction.²⁵ The second step is

Received: September 9, 2014

Revised: October 18, 2014

Published: October 20, 2014

Table 1. List of Sequences^a

Name	Sequence
DI	5'-/Acrydite/-AAAAACAAAGTAGTCTAGGATTCGGCGTG-3' 5'-biotin/-AAAAACAAAGTAGTCTAGGATTCGGCGTG-3'
DM ₁	5'-TTCCCTTATTCTCTCTCCAGTCTAGGATTCGGCGTGGGTTAACACGCCGAATCCTAGACTACTTG-3' 5'-/FAM/-TTCCCTTATTCTCTCTCCAGTCTAGGATTCGGCGTGGGTTAACACGCCGAATCCTAGACTACTTG-3' 5'-/Cy5/-TTCCCTTATTCTCTCTCCAGTCTAGGATTCGGCGTGGGTTAACACGCCGAATCCTAGACTACTTG-3'
DM ₁ (no toehold)	5'-AGTCTAGGATTCGGCGTGGGTTAACACGCCGAATCCTAGACTACTTG-3' 5'-/FAM/-AGTCTAGGATTCGGCGTGGGTTAACACGCCGAATCCTAGACTACTTG-3'
DM ₂	5'-TTAACCCACGCCGAATCCTAGACTCAAAGTAGTCTAGGATTCGGCGTG-3'
Sgc8c aptamer	5'-GAGAGAGAATATAAGGGAAAAAAAAACTAAGTGTACGGTTAGA-3' 5'-/Cy5/-GAGAGAGAATATAAGGGAAAAAAAAACTAAGTGTACGGTTAGA-3'
Scrambled aptamer	5'-GAGAGAGAATATAAGGGAAAAAAAA <u>ACGT</u> CATCCGTAGCGGCATAAGATCGTATGAGATTGACCG-3'
Acrydite-Sgc8c	5'-/Acrydite/-AAAAAAAAATCTAAGTGTACGGTTAGA-3'

^aUnderlined nucleotides denote the scrambled region.

the hybridization of aptamers onto the DNA scaffold. Since each DNA scaffold has multiple sites for aptamer hybridization, the surface can be functionalized with protruding polyvalent aptamers. The synthesis of polyvalent aptamers was evaluated with assays including gel electrophoresis, surface plasmon resonance (SPR), and fluorescence imaging. The polyvalent aptamer-functionalized surface was studied by the examination of cell binding specificity, cell density and cell morphology. Importantly, surfaces with polyvalent or individual aptamers were compared in situations with either equal amounts of ligand display or equal amounts of surface reaction sites.

2. MATERIALS AND METHODS

2.1. Materials. Phosphate buffered saline (PBS), acrylamide/bis(acrylamide), ammonium persulfate, tetramethylethylenediamine (TEMED), acetone, reagent alcohol (91% ethanol), Dulbecco's phosphate buffered saline (DPBS), bovine serum albumin (BSA), glycerol, agarose, tris borate ethylenediaminetetraacetic acid (TBE), glutaric dialdehyde (25 wt % in water), and 1,1,1,3,3-hexamethyldisilazane (HMDS) were purchased from Thermo-Fisher Scientific (Waltham, MA). Sodium hydroxide, glucose, TWEEN 20, and 3-(trimethoxysilyl) propyl methacrylate were purchased from Sigma-Aldrich (St. Louis, MO). Magnesium chloride solution was purchased from ATCC (Manassas, VA) and all oligonucleotides were synthesized by Integrated DNA Technologies (Coralville, IA). For silanization, glass slides were purchased from VWR (Radnor, PA) and base slides for hydrogel synthesis were purchased from Thermo-Fisher Scientific (Waltham, MA).

2.2. Evaluation of Polymerization via Gel Electrophoresis. Prior to polymerization, all monomers and aptamers were heated using a Bio-Rad T100 Thermal Cycler (Hercules, CA) for 3 min at 95 °C and cooled for 1 h to allow sequences to form their most energetically favorable structures. Initiator and monomer sequences were mixed at a 1:10 molar ratio for 1 h at 37 °C for hybridization in a DPBS buffer. Next, aptamer sequences were added to the hybridized DNA solution for 1 h at 37 °C in DPBS. The final monomer-to-aptamer ratio was 1:1. Samples were loaded into the wells of a 1% (*w/v*) agarose hydrogel and run for 50 min at 100 V in TBE running buffer. After electrophoresis, gels were fluorescently imaged using a CRI Maestro In-Vivo imaging system (Woburn, MA). Gel images were processed using Maestro 3.0 software.

2.3. Characterization of Polymerization Using Surface Plasmon Resonance. DNA polymerization was measured using a Reichert Technologies SR7500DC spectrometer, equipped with a SR8100 autosampler (Depew, NY). A biotinylated initiator sequence (1 μM) was flowed over a streptavidin-coated sensor chip (Reichert,

Depew, NY) at 10 μL/min for 10 min. The surface was thoroughly washed to remove loosely bound initiator using both 40 mM NaOH and 1× PBS. To investigate the hybridization of monomers and aptamer to the immobilized initiator, several samples were injected: (1) 2.5 μM DM₂, followed by 2.5 μM aptamer, (2) 2.5 μM DM₁ (without toehold), followed by 2.5 μM aptamer, (3) 2.5 μM DM₁, followed by 2.5 μM aptamer, and (4) 2.5 μM DM₁ + 2.5 μM DM₂, followed by 2.5 μM aptamer. In each case, monomers were injected for 18 min, 45 s at 20 μL/min, followed directly by an aptamer injection for 3 min, 45 s at 20 μL/min and a dissociation period of 10 min using 1× PBS. Between samples, the chip was regenerated at least one time by injecting 40 mM NaOH for 1 min at 20 μL/min with a 2 min dissociation period with 1× PBS. Data was collected using Reichert Technologies SPR Autolink software (Depew, NY). The plotted signal is the difference between analyte and reference channels.

2.4. Measurement of Polymer Extension from a Surface via Dynamic Light Scattering. Streptavidin-coated iron oxide nanoparticles (10 μg, Ocean NanoTech, Springdale, AR) were first washed with buffer (deionized H₂O, 0.1% *v/v* Tween 20) and then mixed with biotinylated DI (1 μM) in 20 μL buffer at room temperature for 1 h on a rotator. After the removal of free DI via centrifugation (14000g for 15 min), nanoparticles were incubated in 100 μL of reaction buffer (PBS with 0.1% *v/v* Tween 20 and 0.02% *w/v* Na₃) containing one or both monomers (each at 2 μM) at room temperature overnight. The nanoparticle solution was purified using Nanosep ultracentrifugal filter (100 kDa cutoff size, Pall Corporation) to remove unreacted monomers and to harvest the nanoparticles. To perform DLS, nanoparticles were dispersed in 1 mL of PBS that was filtered through 0.45 μm membrane (Millipore) prior to use. The nanoparticle dispersions were then transferred to a 12 mm square polystyrene cuvette and were characterized using a Zetasizer ZS (Malvern Instruments, Malvern, Worcestershire, United Kingdom).

2.5. Synthesis of Hydrogel Surfaces. Polyacrylamide hydrogel was coated on the surface of silanized glass squares. Prior to the coating, glass slides were silanized to ensure that the surface of hydrogel was smooth and would not fall off the glass during the operation. Glass microscope slides from VWR (Radnor, PA) were cut into approximately 4 mm × 4 mm squares and sonicated for 15 min in acetone. Following sonication, squares were washed individually with deionized water and dried in a Thermo-Fisher Scientific (Waltham, MA) Isotemp oven for at least 1 h. The squares were immersed in 1 M NaOH and sonicated for 10 min. After squares were washed using deionized water, they were placed in an oven for at least 1 h to dry completely. Silanization solution was prepared as follows in a ventilated chemical hood: 0.5 mL of 3-(trimethoxysilyl) propyl methacrylate was added to 50 mL of ethanol, followed by the addition of 1.5 mL of 10% glacial acetic acid in deionized water. The clean glass

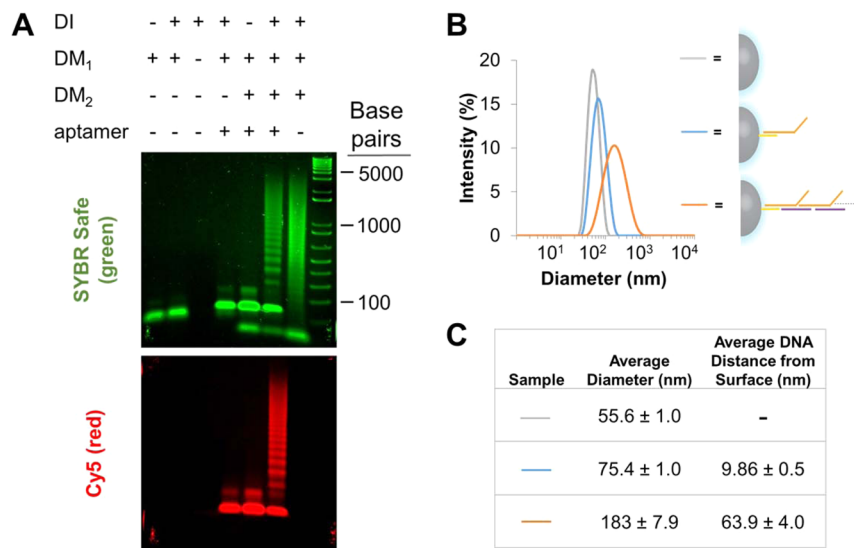


Figure 2. Characterization of DNA polymerization and polyvalent aptamer synthesis. (A) Electrophoretic gel images. The concentration of initiator was 0.3 μM ; the concentrations of DM₁, DM₂, and the aptamer (labeled with Cy5) were all 3 μM . Top image shows SYBR Safe staining (green); bottom image displays the hybridization of the Cy5-labeled aptamer (red) with DNA polymers. (B) Dynamic light scattering plot displays the distribution of particle diameters as a function of DNA length and extension. Nanoparticles were either left bare (gray) or functionalized with initiator and DM₁ (blue) or initiator and DM₁ + DM₂ (orange). (C) Average particle diameter and extension of DNA from the surface were determined from dynamic light scattering analysis. Values include standard deviation ($n = 3$).

squares were immersed in this silanization solution for 5 min and immediately washed with ethanol. After air drying, squares were stored at 25 °C in a desiccator until use. In the case of direct conjugation, 1 μL 10% acrylamide was prepared with a predetermined amount of acrydite-modified aptamer sequence, 0.15 μL of 10% (*w/v*) ammonium persulfate in deionized water, and 0.15 μL of 5% (*v/v*) TEMED in deionized water. This solution was mixed and quickly pipetted to the surface of a clean glass slide. The droplet was immediately covered by a silanized glass square and allowed to polymerize for 1 h at 37 °C in a humid environment. After gel polymerization, the film-coated silanized glass squares were removed from the glass slide base and washed in DPBS. In the case of polyvalent aptamer-functionalized surfaces, 1 μL of 10% acrylamide was prepared with a predetermined amount of acrydite-modified DI, 0.15 μL of 10% (*w/v*) ammonium persulfate in deionized water, and 0.15 μL of 5% (*v/v*) TEMED in deionized water. The gel polymerization procedure was identical to that of directly conjugated aptamer gels. After gel polymerization, samples were washed in DPBS. The polymerization of DNA monomers and aptamer hybridization is detailed in the following section.

2.6. Polymerization of Aptamers on a Hydrogel Surface. Monomers and aptamer were mixed in DPBS to predetermined concentrations and annealed for 3 min at 95 °C in a Bio-Rad T100 Thermal Cycler (Hercules, CA). After allowing 1 h for oligomers to form energetically favorable secondary structures, monomers, and aptamer were ready for sample incubation. For stepwise polymerization, initiator-functionalized hydrogel surfaces were inverted and immersed in 20 μL solutions of alternating monomer solutions at a 1:1 initiator to monomer ratio at 37 °C for 1 h each with wash steps in DPBS between monomer incubations. For simultaneous polymerization, monomers were premixed and initiator-functionalized hydrogel films were inverted and immersed in 20 μL of the monomer mixture for 1 h at 37 °C. After another washing step in DPBS, DNA polymer-functionalized hydrogels were inverted and immersed in 20 μL aptamer or scrambled aptamer solution at a 1:1 aptamer to monomer ratio for 1 h at 37 °C. A final washing step in DPBS was performed to remove any loosely bound aptamer from the polyvalent aptamer-functionalized hydrogel surfaces. Fluorescently labeled monomers and aptamer were examined under an Olympus IX73 inverted microscope equipped with an Olympus U-HGLGPS fluorescence illumination source and an Olympus XM10 camera

(Shinjuku, Tokyo, Japan). CellSens Standard software was used for image acquisition. All error bars represent standard deviation.

2.7. Cell Culture. Two human T cell lymphoma cell lines were cultured: CCRF CEM (ATCC, CCL-199, Manassas, VA) and KARPAS 299 (Sigma-Aldrich, St. Louis, MO). Both cell lines were cultured in RPMI 1640 (ATCC, Manassas, VA) supplemented with 10% fetal bovine serum and 100 IU/mL penicillin/streptomycin (Thermo-Fisher Scientific, Waltham, MA) and incubated at 37 °C, 5% CO₂, in 95% humidity.

2.8. Evaluation of Cell Binding on the Surfaces. For cell capture, hydrogels were incubated in a DPBS binding buffer solution with 10 mM MgCl₂, 4.5 g/L glucose, and 0.1% (*w/v*) BSA, at a concentration of 1 \times 10⁵ cells/mL. Cell incubation occurred for predetermined time periods at 37 °C, 5% CO₂, in 95% humidity. Before imaging, hydrogels were gently shaken for 2 min at 90 rpm to remove unbound cells. Bound cells were examined under an Olympus IX73 inverted microscope equipped with an Olympus XM10 camera (Shinjuku, Tokyo, Japan). CellSens Standard software was used for image acquisition and ImageJ software was used for data analysis. All error bars represent standard deviation.

2.9. Examination of Cell Morphology and Hydrogel Surface via Scanning Electron Microscopy. For scanning electron microscope imaging of cells bound to aptamer-functionalized hydrogels, samples were first fixed to preserve native structures. Hydrogels with cells captured at the surface were first immersed in a 3% (*w/v*) glutaraldehyde in PBS solution for 3 h. Each sample was then rinsed three times in fresh PBS. Next, samples were placed in solutions of ethanol and deionized water varying from 50% (*v/v*) ethanol to 100% ethanol for dehydration. The samples were immersed in 50% ethanol for 15–20 min, followed by 5 min in each solution: 60, 70, 80, and 90% (*v/v*) ethanol in deionized water. In the final dehydration step, samples were immersed in 100% ethanol for 10 min. To dry the samples, the gels were sequentially placed in solutions of 1:1 ethanol/HMDS and 1:2 ethanol/HMDS for 20 min each. Finally, samples were incubated in 100% HMDS overnight. All fixation, dehydration, and drying steps were performed in a ventilated chemical hood. Dry samples were stored in a desiccator until SEM analysis.

2.10. Examination of Film Elasticity. Hydrogels directly conjugated with aptamers or functionalized with polyvalent aptamers were loaded onto the base of an Instron 5966 universal tabletop testing system. Compressive loads were applied at a crosshead speed of

1.3 mm/min to a maximum of 50% compressive strain. The elastic moduli were determined from the slope of stress-strain curves for samples, in triplicate. Bluehill 3.0 software was used to acquire data.

2.11. Determination of Statistical Significance. Statistical significance between mean values was determined using Excel statistical software. A two sample Student's *t* test with *P*-values of ≤ 0.05 was used to indicate statistical significance.

3. RESULTS AND DISCUSSION

3.1. Examination of DNA Polymerization and Aptamer Hybridization. To examine the formation of DNA polymers from oligonucleotides, the size and extension of DNA polymers were studied. In the gel electrophoresis study shown in Figure 2A, fluorescence signals indicate double-stranded DNA (SYBR Safe, green) and Cy5-labeled aptamers (red). Lane 7 shows that DNA polymers could be formed using DI and both DM₁ and DM₂. This is due to the stem-loop structure of the DNA monomers, which extends to a linear structure upon binding with the short, linear DI sequence.

To hybridize the aptamers with the DNA scaffolds, DM₁ was specifically designed with a 25-nucleotide "toehold" region. This design offers versatility to the system, where not only aptamers, but also any affinity ligands modified with sequences complementary to the toehold region can be used to synthesize polyvalent ligand-functionalized surfaces. Moreover, the hybridization of ligands with the DNA scaffold to form polyvalent ligands does not require any harsh chemical reaction conditions. In the electrophoretic gel images, the colocalization of red and green fluorescent species in lane 6 demonstrates that aptamers could hybridize with DNA scaffolds to form polyvalent ligands (Figure 2A).

To examine outward DNA polymer extension from a surface, DLS was employed to measure the hydrodynamic radii of functionalized nanoparticles. To functionalize nanoparticles, they were first treated with initiators and then incubated in solutions of DM₁ or the mixture of DM₁ and DM₂. As shown in Figure 2B,C, nanoparticles were increased by approximately 64 nm in radius upon incubation in a solution with both monomers. Thus, the data suggest that DNA polymers had significant outward growth and extension from the surface, while it is possible for them to flexibly orient at many angles on a surface.

The formation of DNA polymers and polyvalent ligands was also confirmed by SPR analysis (Figure 3). As a mixture of DM₁ and DM₂ was passed over the initiator-functionalized surface, the signal sharply increased in comparison with the signal from only DM₁. This signal increase indicates an increase of mass on the chip surface, clearly showing that DM₁ and DM₂

sequentially hybridized to form DNA polymers. As a control, a solution of only DM₂ was passed over the DI-functionalized surface, resulting in a minimal signal increase and indicating low levels of nonspecific binding. In a second injection step, aptamer solution was passed over the DM₁, DM₂, or DM₁ + DM₂ functionalized chip. The flow of aptamer solution on the DM₁ or DM₁ + DM₂ chip led to an abrupt increase of signal, which shows that aptamers hybridized with DNA monomers or polymers (Figure 3). Additionally, the signal intensity ratio of monomers to polymers was equal to that of monovalent to polyvalent aptamers, suggesting that aptamer hybridization with DNA monomers and polymers was equally efficient. No significant binding of aptamers to the DM₂ control surface was observed, demonstrating the specificity of the aptamer for the binding "toehold" region of DM₁.

3.2. Evaluation of Surface-Displayed DNA Polymers and Polyvalent Aptamers. A polymeric or inorganic surface functionalized with affinity ligands can specifically interact with targets, such as molecules, viruses, microorganisms, or cells, depending on the ligand and application. In this study, we examined cell binding on a polyacrylamide hydrogel. Cell binding was studied as it is important for applications such as cell separation and regenerative medicine;^{23,26} polyacrylamide was used as a model to present polyvalent ligands as it can dramatically minimize nonspecific cell binding.²⁷ To create polyvalent aptamers, initiators were incorporated into polyacrylamide via free radical polymerization (Figure S1). When the initiator-functionalized polyacrylamide was treated with FAM-labeled DM₁ and unlabeled DM₂, it exhibited higher fluorescence intensity than surfaces treated with only FAM-DM₁ (Figure 4A). Minimal fluorescence was observed when surfaces with no initiator were incubated with FAM-DM₁. These results demonstrate that DNA polymers were synthesized on the DI-incorporated polyacrylamide surface. In a similar study, when unlabeled DNA monomers and polymers were formed on a polyacrylamide surface and incubated with Cy5-labeled aptamer, the DNA polymer surfaces exhibited higher fluorescence intensity than control surfaces (Figure 4B). This result indicates that polyvalent aptamers were formed via aptamer hybridization with surface-attached polyvalent DNA scaffolds.

While numerous enzyme-based methods, such as polymerase chain reaction and rolling circle amplification, can in principle be used to synthesize long DNA polymers or nanomaterials for aptamer display,^{22,28,29} the method used herein exhibits two advantages. It does not need any enzymes, which makes the system easier and more robust to use. Moreover, the enzyme-free nature of the present method of DNA polymerization opens an avenue for the incorporation of chemically modified oligonucleotides into DNA polymers. These chemically modified DNA polymers could be used to enhance DNA stability,³⁰ where a DNase-rich environment is required for longer periods of cell catch. The synthesis of chemically modified DNA polymers may be difficult with enzyme-based approaches.

3.3. Examination of Cell Binding on Polyvalent Aptamer-Functionalized Surface. Aptamers are single-stranded oligonucleotides that can, in principle, be selected from synthetic nucleic acid libraries for any targets via SELEX (systematic evolution of ligands by exponential enrichment).^{14,15,31,32} The model aptamer used in this work was originally selected for CCRF-CEM lymphoblastic T-cells by Shangguan et al.^{9,33} Therefore, the capability of aptamer-

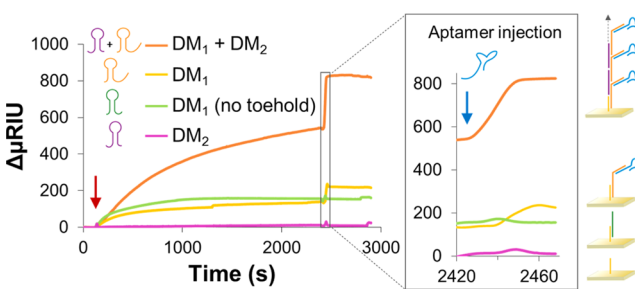


Figure 3. SPR sensorgram displaying DNA polymerization and aptamer hybridization. The red and blue arrows indicate the injections of monomer solutions and aptamer, respectively. Inset displays aptamer injection in greater detail.

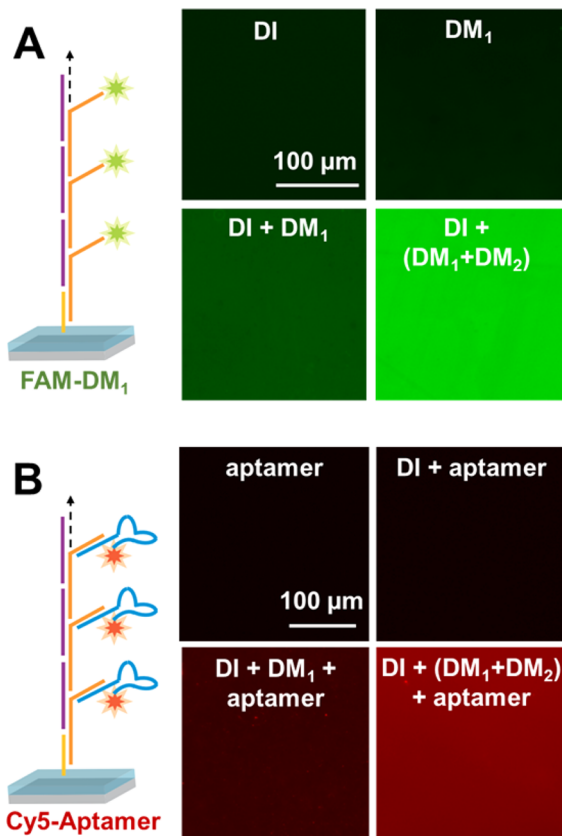


Figure 4. Fluorescence images for demonstration of the formation of (A) DNA polymers and (B) polyvalent aptamers on a hydrogel surface. (A) DI, DI-functionalized hydrogel; DM₁, native hydrogel treated with DM₁; DI + DM₁, DI-functionalized hydrogel treated with DM₁; DI + (DM₁ + DM₂), DI-functionalized hydrogel treated with the mixture of DM₁ and DM₂. DM₁ was labeled with FAM. (B) Aptamer, native hydrogel treated with the aptamer; DI + aptamer, DI-functionalized hydrogel treated with the aptamer; DI + DM₁ + aptamer, DI-functionalized hydrogel treated with DM₁ and the aptamer; DI + (DM₁ + DM₂) + aptamer, DI-functionalized hydrogel treated with the mixture of DM₁ and DM₂ and the aptamer. The aptamer was labeled with Cy5.

functionalized polymeric surfaces to catch cells was examined using the CCRF-CEM cell line.

Polyacrylamide surfaces either were left nonfunctionalized or were functionalized with DNA scaffolds, polyvalent scrambled aptamers, or polyvalent aptamers (Figure 5A). The polymeric surfaces were then incubated with CCRF-CEM cells and imaged to determine the amount of bound cells. The cell binding results for these surfaces show that the cell density on polyvalent aptamer-functionalized surfaces was approximately 800 cells/mm², whereas the cell density on other hydrogel surfaces was less than 5–10 cells/mm² (Figure 5B). These results indicate that the binding functionality of the surface owes directly to aptamer functionalization. Cell binding specificity to aptamer-functionalized surfaces was also examined. Surfaces with polyvalent aptamers were incubated with equal amounts of either control KARPAS 299 cells (control) or target CCRF-CEM cells and compared for cell binding. For KARPAS 299 cells, only 3–5 cells/mm² were observed on the functionalized surface, which was less than 1% of the CCRF-CEM cells observed on an equally functionalized surface (Figure 5C). These data demonstrate that cell binding on the aptamer-functionalized surfaces is specific.

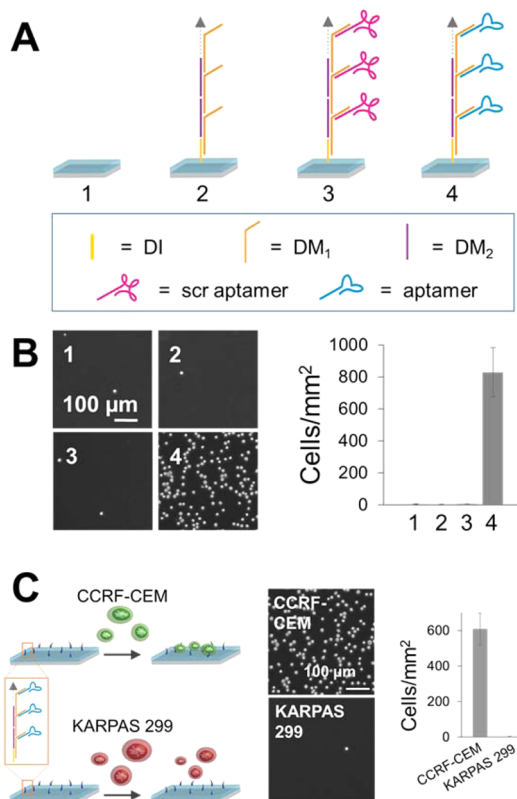


Figure 5. Specific cell binding on the polyvalent aptamer-functionalized surface. (A) Schematic illustration of surface functionalization: (1) blank, (2) polymeric scaffolds, (3) polyvalent scrambled aptamers (scr aptamer), and (4) polyvalent aptamers. (B) Images of cell binding to hydrogels corresponding to samples in (A). (C) Schematic illustration, representative phase micrographs, and analysis of target and control cell binding. $n = 3$ for all experiments.

Previous studies on peptide-functionalized materials indicate that small peptide-based ligands need a spacer to minimize steric hindrance of target binding.³⁴ Since polyvalent aptamers would have further distance from the hydrogel than directly conjugated aptamers, we examined whether the length of a spacer would affect cell binding on an aptamer-functionalized surface. Aptamers were variably spaced from the polyacrylamide surfaces through the stepwise formation of DNA polymers. Only the terminal DM₁ on each polymer contained a “toehold” region, allowing the hybridization of only one aptamer per polymer regardless of polymer length. The results show that the variation of spacer length had negligible effects on cell binding (Figure 6).

The difference between previous findings and our current data may stem from the vicinity of the ligands to the matrix. In previous studies, peptides were made of a few amino acids. Without a spacer, their binding capability may be easily affected by the substrate. Our previous studies have shown that, while aptamers conjugated to substrates with no spacer can bind cells, the cell binding can be increased by adding nucleotide spacers of 5 or 10 nucleotides.²¹ Therefore, the aptamer used in this study with a 10 nucleotide spacer may be sufficient to overcome potential steric hindrance by the substrate.

3.4. Comparison of Direct Conjugation and Polyvalent Display in Situations with Equal Aptamer Amounts. While DNA polymers and polyvalent ligands have been studied for a variety of applications,^{35–38} little attention

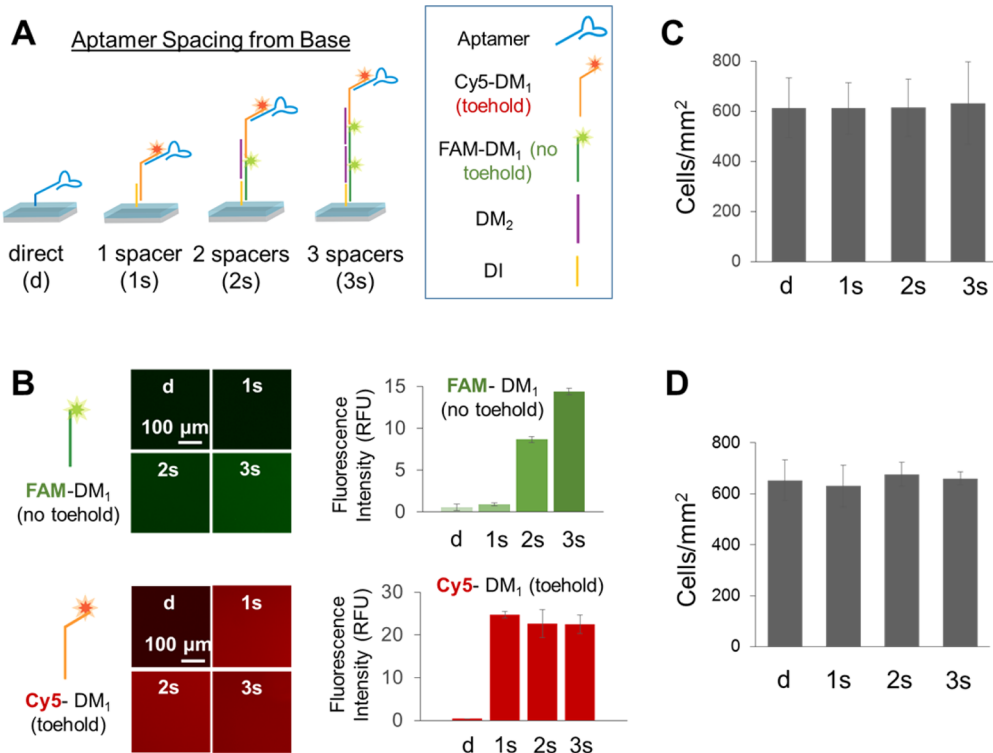


Figure 6. Effects of the length of the linker on aptamer-mediated cell binding. (A) Schematic displaying the spacing of aptamers from the hydrogel surface. Each vertical spacing unit refers to 48 base pairs in the polymer backbone between the surface and the toehold region with aptamer. Aptamers attached directly consist of the cell binding sequence and a 10-nucleotide spacer. (B) Representative fluorescence micrographs and analysis of the monomer fluorescence intensities of stepwise-constructed DNA polymers. Two different DM₁ were used in this study and were labeled with different fluorophores: DM₁ without toehold were labeled with FAM and DM₁ with toehold were labeled with Cy5. (C) Analysis of cells on different surfaces with aptamers variably spaced after 30 min cell incubation or (D) 90 min cell incubation. Error bars represent standard deviation ($n = 3$).

has been paid to the synthesis of DNA-based polyvalent ligands on a surface for the enhancement of ligand display. Therefore, to illustrate the feasibility and advantage of enhanced ligand display on a surface by polyvalent ligands, we designed experiments for two comparisons. Figure 7 is used to compare the effects of direct conjugation and polyvalent display of aptamers on cell binding in situations with equal aptamer amounts on the surface. Figure 7A schematically shows the difference between direct conjugation and polyvalent display when the aptamer amount was 3 \times , 5 \times , or 7 \times . The stepwise polymerization method used to form these surfaces is described in detail in Figure S2. For surfaces with an equal aptamer amount of 7 \times , the results demonstrate that direct conjugation and polyvalent display had little difference in cell binding abilities within the first 30 min of cell incubation (Figure 7B). However, the cell binding capability of polyvalent display was greater when the incubation time reached 90 min or beyond (Figure 7B). Moreover, cell binding reached a maximal level by 30 min with the direct conjugation method whereas it reached a maximal level by 90 min with the polyvalent display method. At 90 min of cell incubation, the polyvalent display of aptamers increased cell binding by 44% in comparison to its direct conjugation counterpart.

To understand whether this difference is a general trend for cell binding on ligand-functionalized surfaces, direct conjugation and polyvalent display were compared in situations with equal aptamer amounts of 3 \times , 5 \times , and 7 \times for cell binding at both 30 and 90 min of cell incubation (Figures 7C and S2). For 30 min cell incubation, direct conjugation and polyvalent display did not exhibit significant differences. However, at 90

min of cell incubation, polyvalent display proved more capable of cell binding than its direct conjugation counterpart in all three aptamer amount groups (3 \times , 5 \times , and 7 \times).

To disclose the potential mechanism, we examined cell morphology under a scanning electron microscope (Figures 8). Some cells appeared to have clear, membranous protrusions as they were bound to surfaces with the direct conjugation of aptamers. This phenomenon was rarely observed on surfaces with the polyvalent display of aptamers. There are two possibilities for these observations. One possibility is that the cells sense and react to the rigidity of the surface. When ligands are directly conjugated to a surface, bound cells are in close proximity to that surface, potentially sensing it. In contrast, the polyvalent display of ligands may allow the cells to be separated from the surface due to increased extension from the surface. Resultantly, the cells may not sense the rigidity of the surface easily. Basic cell biology studies indicate that cells have a tendency to extend and migrate on a highly rigid surface.³⁹ We also examined the morphological and elastic differences between direct conjugation and polyvalent aptamer hydrogels in Figure S3. The results showed no significant differences in sample elasticity. The likely reason for this observation is that the concentrations of DNA or RNA polymers were several orders of magnitude lower than the concentrations of monomers used for hydrogel synthesis. Another possible reason is that DNA polymers on the hydrogel surface may not significantly affect the bulk mechanical properties of the hydrogel. The data also displays no difference in roughness, likely because SEM cannot provide sufficient resolution for detection of nanoscale differences in film roughness. However,

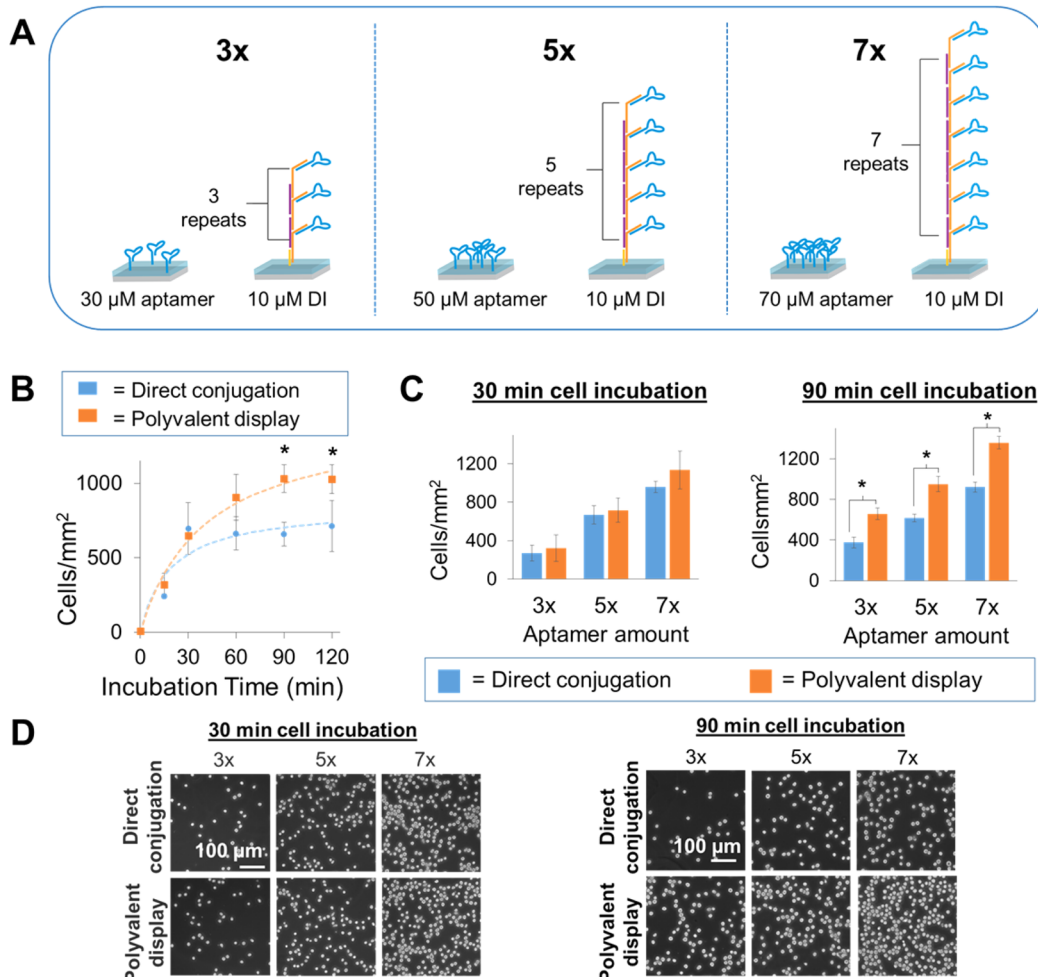


Figure 7. Cell binding on surfaces with equal amounts of aptamer. (A) Schematic comparison of surfaces with equal aptamer amounts. Direct conjugation: individual aptamers were directly conjugated to the hydrogel. Polyvalent display: polyvalent aptamers were formed on the hydrogel surface. (B) Kinetic analysis of cell binding on surfaces with the aptamer amount of 7x. (C) Comparison of cell binding on surfaces with equal amounts of aptamer in three situations, 3x, 5x, and 7x, with representative phase cell images; $n = 3$, * $P \leq 0.05$.

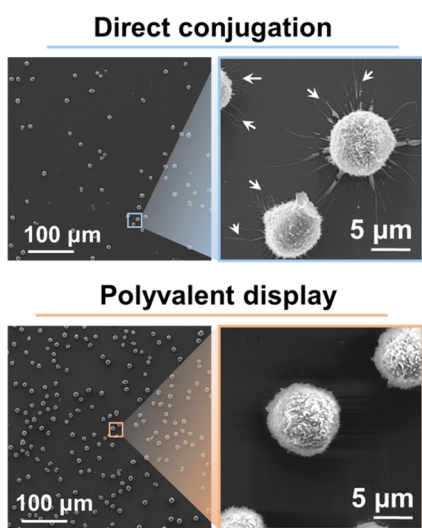


Figure 8. SEM examination of cell morphology. Surfaces with equal aptamer amount (7x) were incubated with cells for 90 min. Arrows point to representative protrusions.

future work can be focused on using more specialized techniques (atomic force microscopy) for a sensitive analysis

of surface mechanical properties and nanoscale morphology. The other possibility is the formation of focal adhesions.^{40–42} With the polyvalent display method, the aptamer units are regularly spaced owing to the stepwise polymerization of the DNA polymeric scaffold. In contrast, with the direct conjugation method, they are randomly distributed on the surface during the free radical polymerization. Thus, the interactions between cell receptors and polyvalent aptamers may lead to stronger focal adhesions. After cell attachment, the next stage is cell migration. The ligand–receptor binding strength is one of the most important factors to determine the potential of cell migration. Previous studies have suggested that cell migration is negatively affected as focal adhesions strength increases.⁴³ As a result, the cells exhibited a higher tendency to develop membranous extensions when binding to the surface with the direct conjugation of aptamers.

While the exact mechanism is unclear and will need more studies in the future, the results indicate that polyvalent aptamers might provide stronger cell binding and suggest that surfaces with polyvalent aptamers would bind more cells than those with the direct conjugation of aptamers in the situation with an equal ligand density.

3.5. Comparison of Direct Conjugation and Polyvalent Display in Situations with Equal Surface Reaction

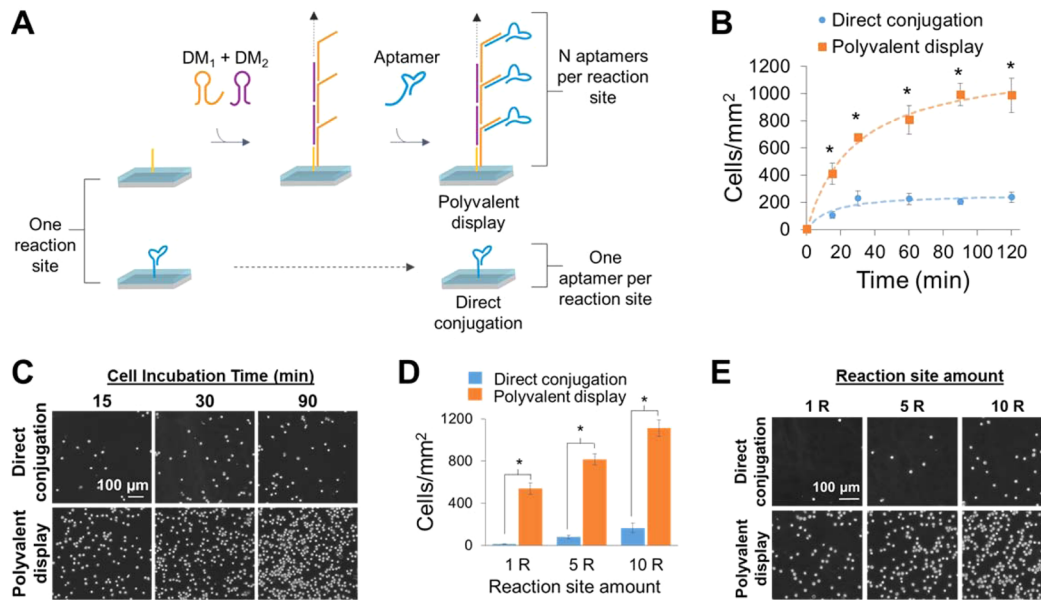


Figure 9. Cell binding on surfaces with equal reaction sites but different aptamer amounts. (A) Schematic illustration of surfaces with equal reaction sites. Each acrydite-aptamer (direct conjugation) or acrydite-DI on the surface presents one reaction site. It is therefore defined that 1 R reaction sites were displayed on the surface when 1 μM acrydite-aptamer or 1 μM acrydite-DI was used to synthesize the hydrogel coating. When 1, 5, and 10 μM acrydite-aptamer or acrydite-DI was used to synthesize hydrogel coatings, surfaces would have reaction sites of 1, 5, and 10 R, respectively. For direct conjugation, 1 R reaction sites displayed 1 R aptamers; for polyvalent display, 1 R reaction sites displayed aptamers of 1 R times N , because the polyvalent aptamer-functionalized surfaces have N aptamers per reaction site. (B) Kinetic analysis of cell binding on hydrogels with 10 R reaction sites. (C) Representative phase micrographs of cell binding on hydrogels with 10 R reaction sites after three incubation time periods. (D) Quantitative comparison of cell binding on hydrogels with 1 R, 5 and 10 R reaction sites. (E) Representative phase micrographs of cell binding in the three situations; $n = 3$, $*P \leq 0.05$.

Sites. We further made another comparison between direct conjugation and polyvalent display in situations with an equal amount of surface reaction sites. Many materials are inert without rich reaction sites. The ability to grow multiple affinity ligands from individual reaction sites would increase the overall valence of the surface compared to the direct conjugation of single ligands to individual reaction sites. Thus, to further demonstrate the advantage of enhanced ligand display, we used the same amounts of acrydite-aptamers and acrydite-DI to synthesize two hydrogels with equal reaction sites (Figure 9A). The DI-functionalized hydrogel was incubated in a solution of DM_1 and DM_2 , and then treated by the aptamer to form polyvalent aptamers. Thus, these two hydrogels have equal reaction sites but different aptamer valences (Figure 9A).

Figure 9B,C shows cell binding kinetics and representative cell images on the surfaces functionalized with the direct conjugation or polyvalent display methods. Polyvalent display led to more cell binding than direct conjugation at all time points. Cell binding reached a maximum capacity of approximately 200 cells/mm² in 30 min when surfaces were directly functionalized with aptamers. In contrast, over 600 cells/mm² were observed on surfaces with polyvalent aptamers in the same period of time. This difference in cell binding became more significant with the increase of cell binding time between 30 and 120 min. We further varied the amounts of reaction sites to examine the difference in cell binding. In all three tested conditions, polyvalent display allowed more cell binding than direct conjugation (Figure 9D,E). The difference was more significant when the amount of reaction sites was lower. Using the polyvalent display method, approximately 40, 10, and 6 times more cells were captured in comparison to the direct conjugation method at reaction site amounts of 1, 5, and

10 R, respectively. These results highlight the advantage of surface functionalization with polyvalent ligands on materials with low or limited amounts of reaction sites via the proposed surface polymerization and ligand display method.

4. CONCLUSIONS

In summary, we have developed a new enzyme-free, DNA-based method for surface functionalization via polymerization of affinity ligands. Surface functionalization with polyvalent ligands enhances ligand display that leads to more cell binding in situations with equal amounts of ligand display or equal amounts of surface reaction sites. While cell binding was studied herein, this enzyme-free, DNA-based surface functionalization method may be applied to improve the binding of other targets, such as small molecules, viruses, or microorganisms, owing to enhanced ligand display. Thus, this study provides a promising platform that may have broad applications where the hurdles of limited surface areas or insufficient surface reaction sites must be overcome.

ASSOCIATED CONTENT

S Supporting Information

Detailed schematics and descriptions of polyvalent aptamer formation. This material is available free of charge via the Internet at <http://pubs.acs.org>.

AUTHOR INFORMATION

Corresponding Author

*Tel.: (814) 865-6867. Fax: (814) 863-0490. E-mail: yxwbiao@engr.psu.edu.

Notes

The authors declare no competing financial interest.

ACKNOWLEDGMENTS

The authors thank Pennsylvania State University Materials Characterization Laboratory for use of their scanning electron microscopes, the Jian Yang lab for use of the compression testing system, and Jinshan Guo for his guidance in compression studies. This work was supported in part by the Penn State Start-Up Fund and the U.S. National Science Foundation (CBET-1340173 and CMMI-1131587). S.L. and N.C. were supported in part by the China Scholarship Council.

REFERENCES

- (1) Chen, C. S.; Mrksich, M.; Huang, S.; Whitesides, G. M.; Ingber, D. E. *Science* **1997**, *276*, 1425–1428.
- (2) Michaud, M.; Jourdan, E.; Villet, A.; Ravel, A.; Grossot, C.; Peyrin, E. *J. Am. Chem. Soc.* **2003**, *125*, 8672–8679.
- (3) Nagrath, S.; Sequist, L. V.; Maheswaran, S.; Bell, D. W.; Irimia, D.; Ulkus, L.; Smith, M. R.; Kwak, E. L.; Digumarthy, S.; Muzikansky, A.; Ryan, P.; Balis, U. J.; Tompkins, R. G.; Haber, D. A.; Toner, M. *Nature* **2007**, *450*, 1235–1239.
- (4) Unruh, D. A.; Mauldin, C.; Pastine, S. J.; Rolandi, M.; Fréchet, J. M. J. *J. Am. Chem. Soc.* **2010**, *132*, 6890–6891.
- (5) Brockman, J. M.; Frutos, A. G.; Corn, R. M. *J. Am. Chem. Soc.* **1999**, *121*, 8044–8051.
- (6) Myung, J. H.; Gajjar, K. A.; Saric, J.; Eddington, D. T.; Hong, S. *Angew. Chem., Int. Ed.* **2011**, *50*, 11769–11772.
- (7) Hong, M.-Y.; Lee, D.; Kim, H.-S. *Anal. Chem.* **2005**, *77*, 7326–7334.
- (8) Frasconi, M.; Tortolini, C.; Botrè, F.; Mazzei, F. *Anal. Chem.* **2010**, *82*, 7335–7342.
- (9) Chen, L.; Liu, X.; Su, B.; Li, J.; Jiang, L.; Han, D.; Wang, S. *Adv. Mater.* **2011**, *23*, 4376–4380.
- (10) Wang, S.; Liu, K.; Liu, J.; Yu, Z. T.-F.; Xu, X.; Zhao, L.; Lee, T.; Lee, E. K.; Reiss, J.; Lee, Y.-K.; Chung, L. W. K.; Huang, J.; Rettig, M.; Seligson, D.; Duraiswamy, K. N.; Shen, C. K.-F.; Tseng, H.-R. *Angew. Chem., Int. Ed.* **2011**, *50*, 3084–3088.
- (11) Liu, B.; Liu, Y.; Riesberg, J. J.; Shen, W. *J. Am. Chem. Soc.* **2010**, *132*, 13630–13632.
- (12) Jayasena, S. D. *Clin. Chem.* **1999**, *45*, 1628–1650.
- (13) Famulok, M.; Hartig, J. S.; Mayer, G. *Chem. Rev.* **2007**, *107*, 3715–3743.
- (14) Tuerk, C.; Gold, L. *Science* **1990**, *249*, 505–510.
- (15) Ellington, A. D.; Szostak, J. W. *Nature* **1990**, *346*, 818–822.
- (16) Chen, N.; Li, S.; Battig, M. R.; Wang, Y. *Small* **2013**, *2*, 1–6.
- (17) Choi, H. M. T.; Chang, J. Y.; Trinh, L. A.; Padilla, J. E.; Fraser, S. E.; Pierce, N. A. *Nat. Biotechnol.* **2010**, *28*, 1208–1212.
- (18) Zhu, G.; Zheng, J.; Song, E.; Donovan, M.; Zhang, K.; Liu, C.; Tan, W. *Proc. Natl. Acad. Sci. U.S.A.* **2013**, *110*, 7998–8003.
- (19) Battig, M. R.; Soontornworajit, B.; Wang, Y. *J. Am. Chem. Soc.* **2012**, *134*, 12410–12413.
- (20) Zhang, Z.; Chen, N.; Li, S.; Battig, M. R.; Wang, Y. *J. Am. Chem. Soc.* **2012**, *134*, 15716–15719.
- (21) Chen, N.; Zhang, Z.; Soontornworajit, B.; Zhou, J.; Wang, Y. *Biomaterials* **2012**, *33*, 1353–1362.
- (22) Zhao, W.; Cui, C. H.; Bose, S.; Guo, D.; Shen, C.; Wong, W. P.; Halvorsen, K.; Farokhzad, O. C.; Teo, G. S. L.; Phillips, J. A.; Dorfman, D. M.; Karnik, R.; Karp, J. M. *Proc. Natl. Acad. Sci. U.S.A.* **2012**, *109*, 19626–19631.
- (23) Wan, Y.; Kim, Y.; Li, N.; Cho, S. K.; Bachoo, R.; Ellington, A. D.; Iqbal, S. M. *Cancer Res.* **2010**, *70*, 9371–9380.
- (24) Myung, J. H.; Gajjar, K. a; Chen, J.; Molokie, R. E.; Hong, S. *Anal. Chem.* **2014**, *86*, 6088–6094.
- (25) Dirks, R. M.; Pierce, N. A. *Proc. Natl. Acad. Sci. U.S.A.* **2004**, *101*, 15275–15278.
- (26) Kilian, K. A.; Mrksich, M. *Angew. Chem., Int. Ed.* **2012**, *124*, 4975–4979.
- (27) Li, S.; Chen, N.; Zhang, Z.; Wang, Y. *Biomaterials* **2013**, *34*, 460–469.
- (28) Chow, D. C.; Chilkoti, A. *Langmuir* **2007**, *23*, 11712–11717.
- (29) Fire, A.; Xu, S.-Q. *Proc. Natl. Acad. Sci. U.S.A.* **1995**, *92*, 4641–4645.
- (30) Verma, S.; Eckstein, F. *Annu. Rev. Biochem.* **1998**, *67*, 99–134.
- (31) Xiao, Z.; Levy-Nissenbaum, E.; Alexis, F.; Lupták, A.; Teply, B. A.; Chan, J. M.; Shi, J.; Digga, E.; Cheng, J.; Langer, R.; Farokhzad, O. C. *ACS Nano* **2012**, *6*, 696–704.
- (32) Wang, J.; Gong, Q.; Maheshwari, N.; Eisenstein, M.; Arcila, M. L.; Kosik, K. S.; Soh, H. T. *Angew. Chem., Int. Ed.* **2014**, *53*, 1–6.
- (33) Shangguan, D.; Li, Y.; Tang, Z.; Cao, Z. C.; Chen, H. W.; Mallikaratchy, P.; Sefah, K.; Yang, C. J.; Tan, W. *Proc. Natl. Acad. Sci. U.S.A.* **2006**, *103*, 11838–11843.
- (34) Hern, D. L.; Hubbell, J. A. *J. Biomed. Mater. Res.* **1998**, *39*, 266–276.
- (35) Bai, W.; Spivak, D. A. *Angew. Chem., Int. Ed.* **2014**, *53*, 2095–2098.
- (36) Xiao, Y.; Piorek, B. D.; Plaxco, K. W.; Heeger, A. J. *J. Am. Chem. Soc.* **2005**, *127*, 17990–17991.
- (37) Zelada-Guillén, G. A.; Riu, J.; Düzung, A.; Rius, F. X. *Angew. Chem., Int. Ed.* **2009**, *48*, 7334–7337.
- (38) Willner, I.; Zayats, M. *Angew. Chem., Int. Ed.* **2007**, *46*, 6408–6418.
- (39) Choquet, D.; Felsenfeld, D. P.; Sheetz, M. P. *Cell* **1997**, *88*, 39–48.
- (40) Plotnikov, S. V.; Pasapera, A. M.; Sabass, B.; Waterman, C. M. *Cell* **2012**, *151*, 1513–1527.
- (41) Ni, Y.; Chiang, M. Y. *Soft Matter* **2007**, *3*, 1285–1292.
- (42) Saez, A.; Ghibaudo, M.; Buguin, A.; Silberzan, P.; Ladoux, B. *Proc. Natl. Acad. Sci. U.S.A.* **2007**, *104*, 8281–8286.
- (43) Palecek, S. P.; Loftus, J. C.; Ginsberg, M. H.; Lauffenburger, D. A.; Horwitz, A. F. *Nature* **1997**, *388*, 537–540.